Simulation of Standing Waves Along a Circular Path

Jason Pruitt
Physics and Astronomy Department, San Jose State University, San Jose, California, USA
(Dated: February 29, 2024)

CONTENTS

I. INTRODUCTION

Understanding waves lends predictive insight into many different physical systems. Since waves are disturbances of media, waves exist in various different forms such as sound, light, and or even as waves in the ocean. Obeying the principle of superposition, two or more traveling waves will add together and interfere either constructively or destructively. Here, the waves either combine to make a larger wave, or annihilate the amplitude. This produces standing waves in the cases that allow for such interactions. Standing waves are a particularly common topic to cover in introductory physics classes, as the exploration of standing waves allows for the explanation of wave behavior inside cavities or along strings and wires - regimes where the ends of a wave are fixed. Musical instruments are a common example of standing waves, where the cavity or strings of an instrument allows the ends of the sound wave to be fixed and produce integer modes of waves.[1] Then, an alteration changes the length of the system to change the allowed fundamental frequencies of the system, as well as the system's fundamental harmonics. Historically, the Bohr model of the atom[2][3] detailed the quantization of angular momentum through standing wave modes along the path of the electron about the nucleus. This suggests the potential for interesting results by investigating standing waves on a circular rather than linear path. We are particularly interested in the modeling of standing waves in this regime since there exists, as our reference Riggs[4] remarks, very few resources on modeling the circular scenario in comparison to those of the linear scenario. This is particularly puzzling given the frequency in which standing waves is mentioned in undergraduate physics classes and demonstrations. Note, however, that this experiment considers the one-dimensional traversal of the wave *along* the circle, unlike the two-dimensional case atop a circular membrane, such as a drum.

II. MODEL

The one-dimensional wave equation is of the form:

$$\frac{\partial^2 \Psi}{\partial t^2} = v\frac{\partial^2 \Psi}{\partial x^2} \tag{1}$$

Where Ψ is the wave function in spatial coordinate x, temporal coordinate t, and with v as the velocity of the wave. Solving the wave equation yields an expression of a traveling wave, written as

$$\Psi_t(x,t) = Asin(k(x - vt)). \tag{2}$$

Where the wave Ψ_t is described by position x and time t, amplitude A, velocity v, the propagation constant (also known as wave number) $k = \frac{2\pi}{\lambda}$, and wavelength λ. The above expression details a wave traveling to the right, whereas

$$\Psi_t(x,t) = Asin(k(x + vt)), \tag{3}$$

describes a wave traveling to the left. Since the two differ only in direction, the interference of the two add to produce a standing wave, of form

$$\begin{aligned}\Psi_{right} + \Psi_{left} &= Asin(k(x - vt)) + Asin(k(x + vt)) \\ &= 2Asin(kx)cos(kvt)\end{aligned} \tag{4}$$

Furthermore, when these two oppositely moving waves come together, the interference interaction between the waves obeys the principle of superposition.

This means that the amplitudes in each region adds together, creating areas of total destructive interference (nodes) and constructive interference (antinodes). Figure 1 below displays the phenomenon as time evolves, as well as the fact that the nodes and antinodes do not change position in time. It is important to note that while no change in x happens for the wave, the amplitude reflects across the x axis. For standing waves, the number of antinodes n in the system is related to the wavelength λ and length L of the system as such

$$n = \frac{2L}{\lambda}, \tag{5}$$

given the ends of the system are fixed.

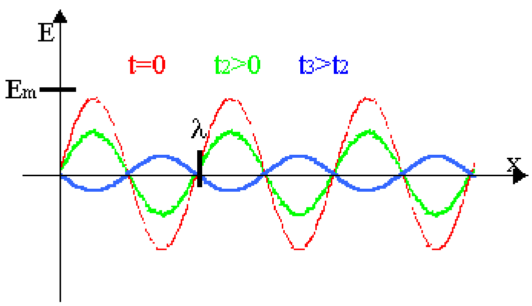

FIG. 1. Time evolution of standing wave. The source[5] considers light waves, hence E_m as the amplitude.

In consideration to time constraints and also personal intrigue, we will attempt to reproduce the results from Rigg's formulation of circular standing waves by solving the advection equation, also known as the "one-way wave equation". The one-dimensional advection equation is of the form

$$\frac{\partial \Psi}{\partial t} = v\frac{\partial \Psi}{\partial x}, \tag{6}$$

which is noticeably similar to the wave equation as we expect.

III. METHODS

We aim to solve the advection equation by comparatively employing both the Lax and Lax-Wendroff methods. Both methods are particularly well suited to solve partial differential equations (PDEs) as they are a modification of

$$\Psi_i^{n+1} = \Psi_i^n - \frac{c\Delta t}{\Delta x}(\Psi_{i+1}^n - \Psi_{i-1}^n), \tag{7}$$

the forward-time center-space (FTCS) finite difference method. The FTCS method for the advection equation is unfortunately unconditionally unstable, meaning it produces compounding errors regardless of how incrementally small or large the steps taken are. The Lax method is a modification of the FTCS scheme that aims to "damp" out such instability by sampling points around each index, and takes the form

$$\Psi_i^{n+1} = \frac{1}{2}(\Psi_{i+1}^n + \Psi_{i-1}^n) - \frac{c\Delta t}{\Delta x}(\Psi_{i+1}^n - \Psi_{i-1}^n), \tag{8}$$

The Lax-Wendroff method is a further improvement derived from a second order Taylor expansion. This reformation attempts to employ a less aggressive damping factor to combat instability, and is of the form

$$\begin{aligned}\Psi_i^{n+1} &= \Psi_i^n - \frac{1}{2}(\frac{c\Delta t}{\Delta x})(\Psi_{i+1}^n + \Psi_{i-1}^n) \\ &+ \frac{1}{2}(\frac{c\Delta t}{\Delta x})^2(\Psi_{i+1}^n - \Psi_{i-1}^n - 2\Psi_i^n),\end{aligned} \tag{9}$$

The experiment simulates right and left moving waves (counterclockwise and clockwise along the circle) in order to investigate the Lax and Lax-Wendroff methods' abilities to reproduce standing wave from the advection equation for waves along the circular path. As a method of verification, we fit the numerical data from the two methods to an analytical solution. To fit a sinusoidal function to the data, we used lmfit.models.ExpressionModel() to pass in a string of our expression. This function builds a model from the string rather than a python function detailing the inputs, and allows for handling of nonlinear fitting functions. The ExpressionModel() object has a method make_params() that allows for parameter creation based off of the string passed into the model's creation.

IV. RESULTS

A. Reproduction of Bohr Model Figure

The solutions of the advection equation from the Lax-Wendroff method take the form from Riggs' figure of the Bohr atomic model. We produce plots for each value of antinodes that reproduce the figures displayed in Figure 2. The main results of the experiment are displayed in Figures 3-7.

Of note is the fact that the Lax method's damping factor is much too strong and causes the solution to collapse to a value equal to the radius of the circle at all times. Analogously, this is as if the solution

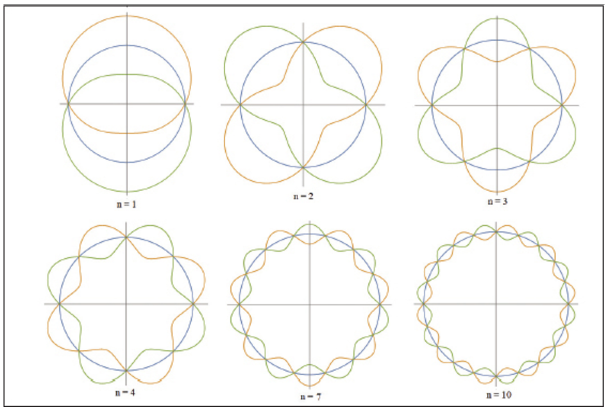

FIG. 2. Riggs' Figure of the Bohr Atomic Model

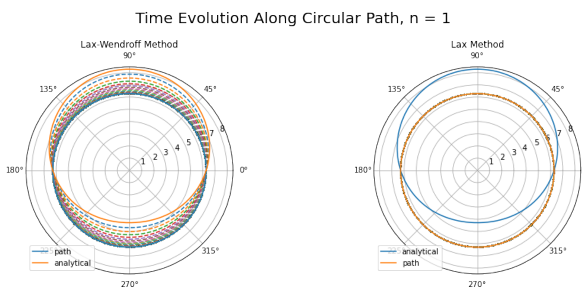

FIG. 3. Lax-Wendroff (left) and Lax (right) solutions to the 1-D Advection Equation for counterclockwise and clockwise waves around the circular path, n = 1 referring to the number of antinodes

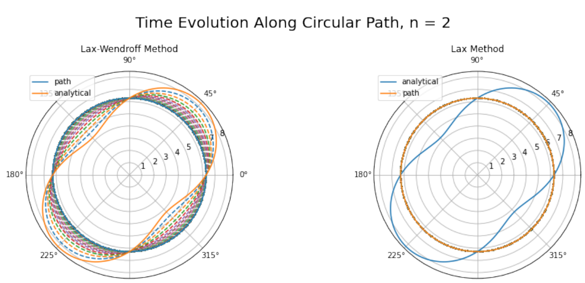

FIG. 4. Lax-Wendroff (left) and Lax (right) solutions to the 1-D Advection Equation for counterclockwise and clockwise waves around the circular path, n = 2 referring to the number of antinodes

went to zero at all times for the linear case. We suspect that the reason the Lax-Wendroff is able to produce solutions while the Lax method is not is due to fact that the damping factor is less aggressive as a result of the contribution from the higher order terms in the Taylor expansion. Additionally, the number of antinodes in the Lax-Wendroff solutions seems to be double the value of n, rather than the linear case where the value of n detailed the number

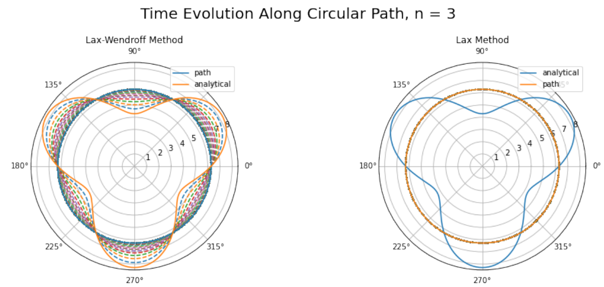

FIG. 5. Lax-Wendroff (left) and Lax (right) solutions to the 1-D Advection Equation for counterclockwise and clockwise waves around the circular path, n = 3 referring to the number of antinodes

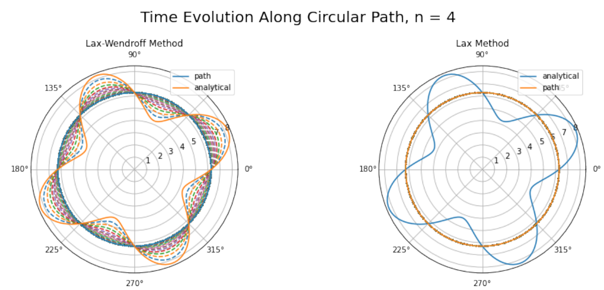

FIG. 6. Lax-Wendroff (left) and Lax (right) solutions to the 1-D Advection Equation for counterclockwise and clockwise waves around the circular path, n = 4 referring to the number of antinodes

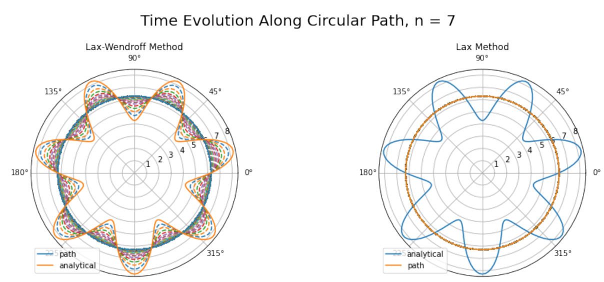

FIG. 7. Lax-Wendroff (left) and Lax (right) solutions to the 1-D Advection Equation for counterclockwise and clockwise waves around the circular path, n = 7 referring to the number of antinodes

of antinodes in the system.

B. Traveling vs. Standing Waves on Circular Paths

Riggs is careful to differentiate between waves simply traveling along a circle and waves that produce the phenomenon of standing waves. As Riggs mentions, the locations of the nodes and antinodes of a

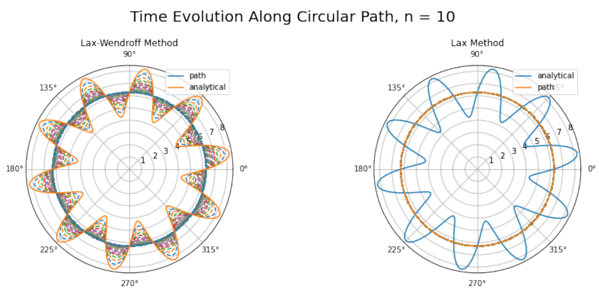

FIG. 8. Lax-Wendroff (left) and Lax (right) solutions to the 1-D Advection Equation for counterclockwise and clockwise waves around the circular path, n = 10 referring to the number of antinodes

traveling wave change over time, whereas these locations do not change for a standing wave and remain the same throughout time. As the Lax-Wendroff method iterates through time, we notice the data follows this. This leads us to conclude that we partially reproduce the behavior of standing waves, without the reflection of antinodes across the path. We hypothesize that this is either the result of the difference between the wave and advection equations, or the lack of boundary conditions to ensure proper reflection of the wave back through the system. This is further corroborated by our attempt to fit to an analytical solution. If attempting to implement boundary conditions, the linear case suggests that Dirichlet Boundary conditions would be appropriate to affix the value of the wave as it approaches the boundaries.

C. Fitting/Comparison to Theoretical Expectation

To compare our results to an analytical solution, we employed LMFIT to see how the numerical solution evolved with time. We examined the time evolution of the Lax-Wendroff solutions by fitting our equation for a standing wave to the numerical data and seeing the change in amplitude each iteration, shown in Figures 9 and 10. While we initially might guess that the model is potentially overfitting the data, it is reasonable that the stable solutions from the Lax-Wendroff method return very high goodness of fit metrics when compared to a sinusoidal function. Unsurprisingly, we also obtain high goodness of fit metrics from the Lax method, but this is due to the fact that the method collapses the initial condition to the circle radius, and so we expect the metrics related to the Lax method's fit to the analytical solution to remain constant throughout time. Figure 9 shows the solution at time = 0 and Figure 10 shows the solution two timesteps later. When first attempting to fit the solution at each timestep to a sinusoidal function $C + Asin(nx)cos(nt)$ (similar to equation 4) with LMFIT, we noticed the Lax-Wendroff solution's amplitude to decay over time. Plotting the decay in amplitude versus iteration number, we notice that the amplitude reduces to the circle's radius (zero in the linear analogue) displayed in Figure 11. We attempted to fit this decay to a number of LMFIT's built in functions that might represent this behavior, but this proved too difficult to finish within the given time.

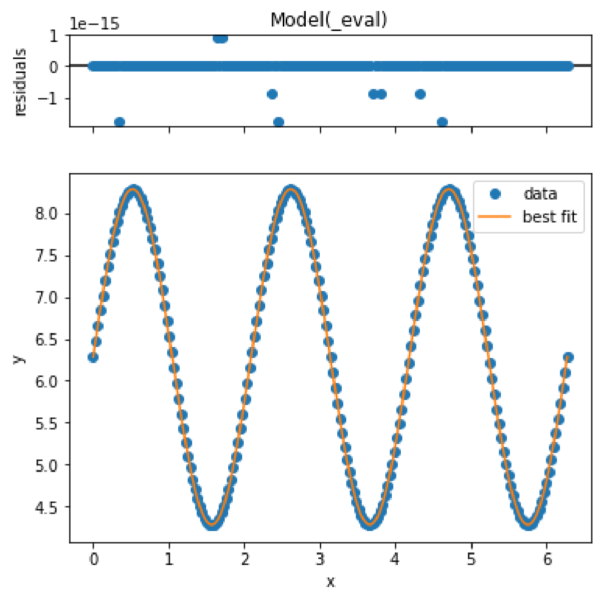

FIG. 9. Fit of $C + Asin(nx)cos(nt)$ with LMFIT at t=0

While the amplitude does decay down to the circle radius, we do note that sending a wave of negative amplitude produces the other half of the graph that we expect to see. This further supports the idea that the behavior exhibited is as a result of the differences between the wave and advection equations. This is displayed in Figure 12.

D. Investigating Different Initial Conditions

In addition to two waves going in different directions, we also implemented a singular sinusoidal initial condition, given by

$$\Psi(x, 0) = sin(\frac{2n\pi x}{L}), \tag{10}$$

with L being the length of the system in the linear case, or the circumference of the circle. Finally, we implemented a third initial condition of a Gaussian pulse described by

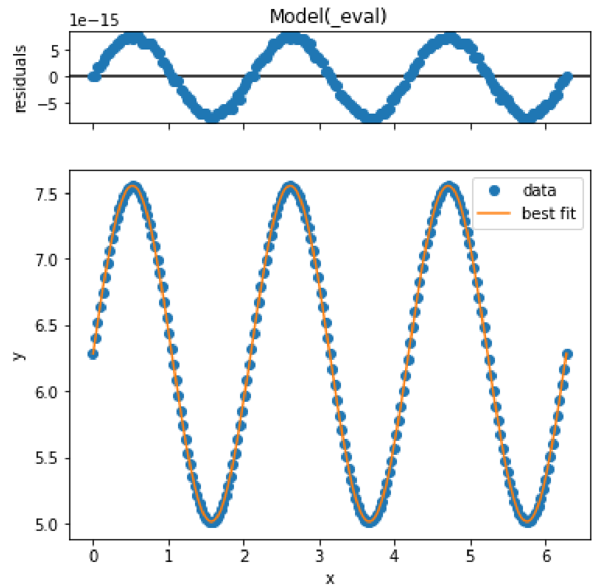

FIG. 10. Fit of $C + Asin(nx)cos(nt)$ with LMFIT at t=2

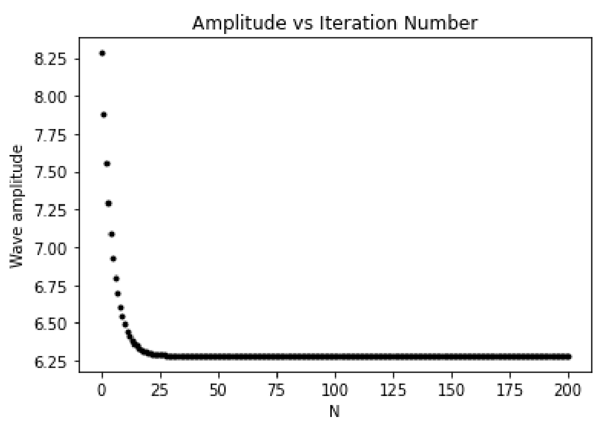

FIG. 11. The decay of wave amplitude as a function of iteration number

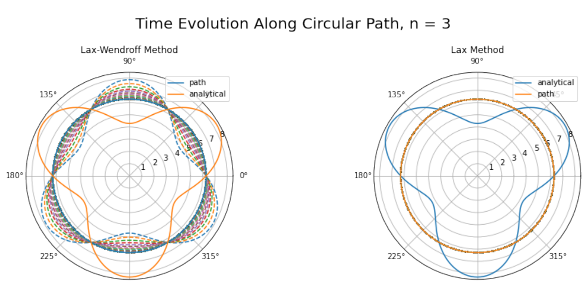

FIG. 12. Sending waves of opposite/negative amplitude produces the other half of the standing wave that is not seen previously, counterclockwise and clockwise waves with n=3

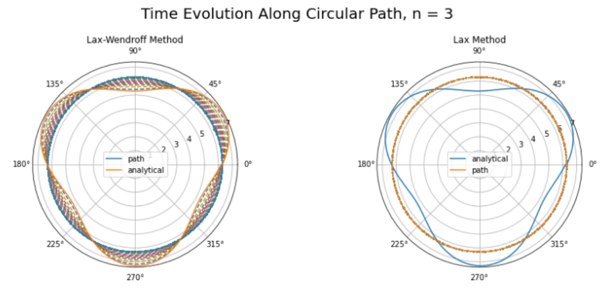

FIG. 13. Lax-Wendroff (left) and Lax (right) solutions to the 1-D Advection Equation for a single sine wave around the circular path, n = 3 referring to the number of antinodes

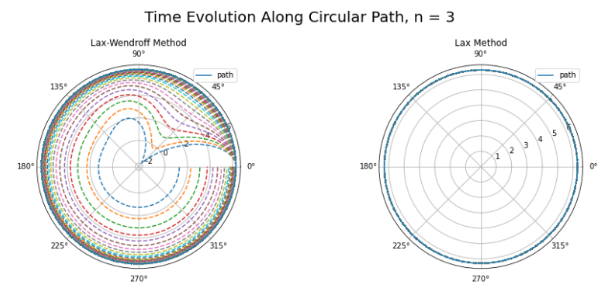

FIG. 14. Lax-Wendroff (left) and Lax (right) solutions to the 1-D Advection Equation for a gaussian pulse around the circular path, n = 3 irrelevant

$$\Psi(x,0) = cos(\frac{\pi x}{\sigma})e^{\frac{-x^2}{2\sigma^2}}, \tag{11}$$

where σ is the width of the pulse. The sine condition is displayed in Figure 13 and the gaussian in Figure 14.

The single sine wave appears to be very similar to the standing wave candidate solutions from earlier, with less amplitude shown around the same antinodes. The initial condition produces very nearly the same shape, just less pronounced. This makes sense as there is only one wave in the system rather than two that can contribute. The gaussian pulse is very ill behaved and decays to the radius of the circle. We are unsure of what physical system this could represent - or potentially if the implementation is incorrect and cannot be conclusive.

V. CONCLUSIONS

Overall, this project has proved to be an excellent opportunity to comparatively employ two different PDE solving methods. We can conclude that the

Lax-Wendroff method outperforms the Lax method in solving the 1-D advection equation along a circle. We have partially reproduced the behavior of standing waves in a circular regime and investigated different initial conditions for the same system. As for other key takeaways, the simplification to use the advection equation in place of the wave equation did prove a barrier in reproducing the full behavior of standing waves. The in class notes mention two possible alternative approaches, where the wave equation may be better solved using either spectral methods, or casting the problem into a flux-conservation formulation. The comparison of these two methods would also prove to be an interesting endeavor as well, but the flux-conservation formulation would still allow for the use of the Lax-Wendroff method, for which we produced hopeful results.

[1] Richard E Berg. Overtones. https://www.britannica.com/science/sound-physics/Overtones.

[2] Danning Bloom and Dan W. Bloom. Vibrating Wire Loop and the Bohr Model. *The Physics Teacher*, 41(5):292–294, 05 2003.

[3] John Daintith. Bohr theory. https://www.oxfordreference.com/view/10.1093/oi/authority.20110803095515653.

[4] Peter Riggs. Revisiting standing waves on a circular path. *The Physics Teacher*, 59(2):100–102, 02 2021.

[5] Doris Jeanne Wagner. Introduction to standing light waves. https://www.rpi.edu/dept/phys/ScIT/InformationTransfer/standwave/standing_waves.html.